

LETTERS

## Extending the correlation of $L_R - L_X$ to gamma-ray bursts \*

Jing Lü<sup>1,2</sup>, Jing-Wen Xing<sup>3</sup>, Yuan-Chuan Zou<sup>3</sup>, Wei-Hua Lei<sup>3</sup>, Qing-Wen Wu<sup>3</sup> and Ding-Xiong Wang<sup>3</sup>

<sup>1</sup> GXU-NAOC Center for Astrophysics and Space Sciences, Department of Physics, Guangxi University, Nanning 530004, China

<sup>2</sup> Guangxi Key Laboratory for Relativistic Astrophysics, Nanning 530004, China

<sup>3</sup> School of Physics, Huazhong University of Science and Technology, Wuhan 430074, China; zouyc@hust.edu.cn

Received 2015 February 8; accepted 2015 March 15

**Abstract** The well-known correlation between radio luminosity ( $L_R$ ) and X-ray luminosity ( $L_X$ ),  $L_R/L_X \simeq 10^{-5}$ , holds for a variety of objects, such as active galactic nuclei, Galactic black holes, solar flares and cool stars. Here we extend the relation to gamma-ray bursts (GRBs) and find that the GRBs also obey a similar  $L_R - L_X$  relation, with a slightly different slope of  $L_R \propto L_X^{1.1}$ . This relation implies that the explosions that occur on different scales may have a common underlying origin.

**Key words:** gamma-ray bursts: general — quasars: general — stars: black holes

### 1 INTRODUCTION

With the enhancement of observational instruments, continuum radiation ranging from radio wavelengths to X-rays has been observed from more and more astronomical objects, such as active galactic nuclei (AGNs) (Sanders et al. 1989; Merloni et al. 2003), the Sun, cool stars (Guedel & Benz 1993), X-ray binaries (Gallo et al. 2003) and gamma-ray bursts (GRBs) (Kumar & Zhang 2014, for a recent review). Recently, the relation between radio and X-ray emission among objects that have different scales has attracted much attention. The radio flares and soft X-rays from the dwarf M-star UV Ceti were observed simultaneously by both VLA and the ROSAT/HRI telescope respectively (Benz et al. 1996). For active cool stars, Guedel & Benz (1993) obtained a tight correlation between the quiescent radio and X-ray emission, where  $L_R/L_X \sim 10^{-5}$ , known as the Güdel-Benz relation. During the ROSAT All-Sky Survey accompanied by mostly simultaneous VLA observations, Guedel et al. (1993) also found a tight correlation between radio and X-ray luminosities of M dwarfs. Benz & Guedel (1994) showed the soft X-ray and radio luminosities of solar flares and the coronae of main-sequence, late-type stars follow the relation  $L_{\nu, X}/L_{\nu, R} = k \times 10^{15.5 \pm 0.5}$ , where  $k$  is a coefficient and different types of stars have different values. Linsky (1996) suggested that the heating mechanism of the stellar corona is a flare-like process, and in a review, van den Oord (1999) discussed various aspects of stellar flares. Guedel (1996) discussed a few aspects of radio and X-ray studies of solar-like stars and showed that nonthermal radio and thermal soft X-ray emissions from solar-like stars provided direct information on particle acceleration and coronal heating in the magnetically confined outer atmospheres. Laor & Behar (2008) found that there is a tighter

---

\* Supported by the National Natural Science Foundation of China.

correlation between the radio and X-ray fluxes of accretion disks in radio-quiet quasars (RQQs) than in coronally active stars,  $L_R/L_X \lesssim 10^{-5}$  (with a  $1\sigma$  scatter of about a factor of 3 in  $L_R$ ). They proposed that most of the radio emission might come from the coronae and that the coronae are magnetically heated. Middleton et al. (2013) showed that the X-ray and radio emission are coupled in some sources. Continued radio and X-ray observations of some sources should reveal the causal relationship between the accretion flow and the powerful jet emission. Here we try to extend the  $L_R - L_X$  relation to GRBs.

GRBs are high energy  $\gamma$ -rays lasting from several milliseconds to a few thousand seconds, and they are the most powerful explosions in the universe (Piran 2004; Zhang 2007). GRBs were discovered in the late 1960s by Vela satellites that were used for monitoring possible nuclear explosions (Klebesadel et al. 1973), and subsequently attracted great interest by astronomers. Because the duration of a GRB explosion is very short, its precise location cannot be determined at the beginning. Not until after the BeppoSAX satellite was launched on 1996 April 30 was the cosmological distance of GRBs confirmed in 1997 (see Kumar & Zhang 2014, for a review of GRBs). With the launching of more space missions with similar objectives (such as *Swift* and *Fermi*), our knowledge about this phenomenon has been greatly enriched. With more and more observational data, statistical studies have revealed some empirical relationships, such as  $E_{\text{peak}} \sim E_{\gamma,\text{iso}}$  (Amati et al. 2002),  $E_{\text{peak}} \sim L_{\gamma,\text{iso}}$  (Yonetoku et al. 2004),  $E_{\text{peak}} \sim E_{\gamma}$  (Ghirlanda et al. 2004),  $E_{\text{peak}} \sim E_{\gamma,\text{iso}} \sim t_b$  (Liang & Zhang 2005),  $L_X - T_a - E_{\gamma,\text{iso}}$  (Xu & Huang 2012),  $z - \alpha$  (Geng & Huang 2013),  $\Gamma_0 \sim E_{\gamma,\text{iso}}$  (Liang et al. 2010) and  $\Gamma_0 \sim L_{\gamma,\text{iso}}$  (Ghirlanda et al. 2012; Lü et al. 2012). A dedicated theoretical study of the  $\Gamma_0 - L_{\gamma,\text{iso}}$  relation has suggested that this relation can be the theoretical justification for central engine models in GRBs (Lei et al. 2013).

Recently, Wu et al. (2011) found a uniform correlation between the synchrotron luminosity and Doppler factor of both GRBs and blazars, which implies that they may share some similar jet physics. The recent work by Wang et al. (2014b) on Sw J1644+57 (a candidate of a tidal disruption event which ejected a relativistic jet) may support this similarity. In their work, the radio light curves of Sw J1644+57 were successfully interpreted with the afterglow jet model. Wang et al. (2014a) found the GRBs and blazars may share a common process that generates radiation. This is apparent from the common correlation between the radio luminosity and broadband spectral slope  $\nu L_{\nu}(5 \text{ GHz}) - \alpha_{\text{RX}}$ , and the radio luminosity and radio peak energy  $\nu L_{\nu}(5 \text{ GHz}) - \nu_{\text{peak}}$ . The discovery of the long-lived afterglows at X-ray, optical and radio wavelengths advanced the study of large samples of GRBs. Chandra & Frail (2012) provided a catalog of radio afterglows corresponding to GRBs over a 14 year period from 1997 to 2011, and also included the 11 h X-ray observations in it. These progresses make it possible to extend the  $L_R - L_X$  relation to GRBs. Currently, the number of GRBs with radio afterglow observations is still small. China's radio telescope FAST, which is under construction, may help to change this situation. Recently, the ability of FAST to detect radio afterglows was studied by Zhang et al. (2015), which concluded that FAST will be able to detect radio afterglows of GRBs typically to redshift  $z = 5$ .

This paper is organized as follows. In Section 2, we describe the selection of samples and analysis of solar flares, cool stars, AGNs and GRBs data. We end with a brief conclusion and discussion in Section 3.

## 2 DATA AND ANALYSIS

We investigate the  $L_R - L_X$  relation of objects with different scales, including stars, AGNs and GRBs. The data on solar flares and cool stars are taken from Laor & Behar (2008). The radio and X-ray data were acquired simultaneously. Soft X-rays from solar flares are conventionally measured in a narrow and harder band than those from stellar sources, and the data points representing solar flares are from different classes that may deviate from the overall linear relation (Benz & Guedel

1994). We take the  $L_R$  and  $L_X$  of AGNs from Merloni et al. (2003), with 5-GHz core emission for the radio luminosity and the 2–10 keV band for the X-ray luminosity.

Our analysis focuses on  $L_R$  and  $L_X$  for GRBs. Based on the radio peak flux densities and luminosity distances  $D_L$  calculated from the redshift  $z$ , we can obtain the radio luminosity of GRB afterglows by  $L_R \simeq 4\pi D_L^2 F_{\nu,m} \times \nu_R$ . For GRBs, we choose 47 samples with both radio and X-ray observations. They are listed in Table 1. Prior to GRB 111215A, the 42 GRBs are taken from Chandra & Frail (2012), who have collected all the radio observations of GRB afterglows. The radio frequency and peak flux densities are listed in their table 3, and X-ray fluxes at 11 h after the burst

**Table 1** Quantities related to GRBs. The X-ray data are taken from the official website of *Swift* while the radio data are taken from the references listed below.

GRB	$z$	$D_L$ (Mpc)	$\nu_R$ (GHz)	$F_m$ ( $\mu$ Jy)	$F_R$ ( $10^{-20}$ erg cm $^{-2}$ s $^{-1}$ )	$F_X^{11h}$ ( $10^{-13}$ erg cm $^{-2}$ s $^{-1}$ )	$L_R$ ( $10^{40}$ erg s $^{-1}$ )	$L_X$ ( $10^{45}$ erg s $^{-1}$ )	Ref.
970508	0.835	5299.32	8.46	958	8.10	5.7	27.23	1.92	[1]
970828	0.958	6288.80	8.46	144	1.22	19.9	5.76	9.42	[1]
980425	0.009	38.27	8.64	39360	340.07	2.8	0.060	0.000049	[1]
980703	0.966	6354.40	8.46	1370	11.59	14.0	56.0	6.76	[1]
981226	1.110	7558.88	8.46	137	1.16	2.8	7.92	1.91	[1]
990510	1.619	12108.32	8.46	255	2.16	34.7	37.84	60.87	[1]
991216	1.020	6800.95	15.00	1100	16.50	78.1	91.31	43.22	[1]
010222	1.477	10800.10	8.46	93	0.79	70.5	10.98	98.39	[1]
011211	2.140	17105.31	8.46	162	1.37	180.0	47.98	630.15	[1]
021004	2.330	18991.03	22.50	1614	36.32	8.4	1567.09	36.25	[1]
030226	1.986	15599.76	22.50	328	7.38	13.5	214.88	39.31	[1]
030329	0.169	804.57	43.00	59318	2550.67	548.6	197.56	4.25	[1]
031203	0.105	479.23	22.50	483	10.87	4.5	0.30	0.012	[1]
050401	2.898	24785.55	8.46	122	1.03	35.1	75.86	258.00	[1]
050416A	0.650	3887.37	8.46	373	3.16	25.3	5.71	4.57	[1]
050525A	0.606	3566.96	8.46	164	1.39	51.5	2.11	7.84	[1]
050603	2.821	23987.77	8.46	377	3.19	33.0	219.59	227.20	[1]
050730	3.968	36185.46	8.46	212	1.79	76.7	280.99	1201.64	[1]
050820A	2.615	21871.45	8.46	150	1.27	221.2	72.63	1266.05	[1]
050824	0.830	5259.90	8.46	152	1.29	13.7	4.26	4.54	[1]
050904	6.290	62311.66	8.46	76	0.64	0.5	298.70	23.23	[1]
051022	0.809	5095.05	8.46	268	2.27	426.5	7.04	132.47	[1]
060218	0.033	142.97	22.5	250	5.63	48.8	0.014	0.012	[1]
060418	1.490	10918.75	8.46	216	1.83	9.4	26.07	13.41	[1]
070125	1.548	11450.89	22.50	1778	40.01	37.8	627.63	59.30	[1]
071003	1.604	11968.90	8.46	616	5.21	55.7	89.32	95.47	[1]
071010B	0.947	6198.94	8.46	341	2.89	45.6	13.26	20.97	[1]
071020	2.146	17164.39	8.46	141	1.19	16.1	42.05	56.75	[1]
080603A	1.687	12743.86	8.46	207	1.75	15.8	34.03	30.70	[1]
090313	3.375	29800.55	8.46	435	3.68	31.9	391.04	338.96	[1]
090323	3.570	31883.30	8.46	243	2.06	28.1	250.04	341.78	[1]
090328	0.736	4531.37	8.46	686	5.80	61.4	14.26	15.08	[1]
090423	8.260	85417.81	8.46	50	0.42	5.0	369.27	436.49	[1]
090424	0.544	3126.69	8.46	236	2.00	2.3	2.34	0.27	[1]
090715B	3.000	25847.66	8.46	191	1.62	8.2	129.17	65.55	[1]
090902B	1.883	14605.36	8.46	84	0.71	47.0	18.14	119.96	[1]
091020	1.710	12960.08	8.46	399	3.38	19.5	67.84	39.19	[1]
100414A	1.368	9814.85	8.46	524	4.43	143.7	51.10	165.63	[1]
100418A	0.620	3668.21	8.46	1218	10.30	10.7	16.59	1.72	[1]
100814A	1.440	10463.72	7.90	613	4.84	82.0	63.44	107.42	[1]
100901A	1.408	10174.38	33.60	378	12.70	90.1	157.31	111.60	[1]
100906A	1.727	13120.28	8.46	215	1.82	27.1	37.46	55.82	[1]
111215A	2.060	16320.50	8.40	1340	11.26	140.0	358.73	446.30	[2, 3]
120326A	1.798	13792.90	15.00	771	11.57	93.2	263.25	212.10	[4, 5]
130427A	0.340	1783.10	15.70	4183	65.67	2167.6	24.98	82.46	[6, 7, 8]
130603B	0.3565	1882.80	6.70	118.6	0.79	8.5	0.34	0.36	[9, 10]
130907A	1.238	8663.80	15.00	1060	15.90	308.1	142.80	276.74	[11, 12]

Notes: [1] Chandra & Frail (2012); [2] van der Horst et al. (2015); [3] Zauderer et al. (2013); [4] Kruehler et al. (2012); [5] Staley et al. (2013); [6] Xu et al. (2013); [7] Flores et al. (2013); [8] Anderson et al. (2014); [9] Cucchiara et al. (2013); [10] Fong et al. (2014); [11] de Ugarte Postigo et al. (2013); [12] Veres et al. (2014).

are listed in their table 6. There are five remaining radio afterglows that were subsequently observed and described in various references. For these five GRBs in our sample, the references are listed in the following. GRB 111215A: van der Horst et al. (2015) for the redshift and Zauderer et al. (2013) for the radio peak flux density. In figure 3 of Zauderer et al. (2013), there are five radio light curves at 5.8, 8.4, 19.1, 24.4 and 93 GHz, but from their profiles, the first three may result from the reverse and forward shocks, and the remaining two may result from external shocks, so we chose the peak flux density of 8.4 GHz. GRB 120326A: Kruehler et al. (2012) for the redshift and Staley et al. (2013) for the radio peak flux density. GRB 130427A: Xu et al. (2013) and Flores et al. (2013) for the redshift and Anderson et al. (2014) for the radio peak flux density. GRB 130603B: Cucchiara et al. (2013) for the redshift and Fong et al. (2014) for the radio peak flux density. GRB 130907A: de Ugarte Postigo et al. (2013) for the redshift and Veres et al. (2014) for the radio peak flux density. The X-ray fluxes at 11 h after these five bursts are taken from the official website of *Swift* XRT data for GRBs in the range 0.3–10 keV<sup>1</sup>.

In Figure 1, we show the distribution of the 15 solar flares (from Laor & Behar 2008), 65 cool stars (from Laor & Behar 2008), 149 AGNs (from Merloni et al. 2003) and 47 GRBs (from Table 1) in the  $L_R - L_X$  plane. The black solid line in the lower panel, which traces the relation  $L_{R,40} \simeq 10.6L_{X,45}^{1.1}$ , is the best fit and can be compared to the red dashed line that follows the relation  $L_R = 10^{-5}L_X$ . Remarkably, both of them appear to follow a similar  $L_R - L_X$  relation, despite the fact that they span  $\sim 30$  orders of magnitude in luminosity between these different types of active objects.

We investigate the  $L_R - L_X$  relation mentioned by Benz & Guedel (1994) with our larger samples. Laor & Behar (2008) obtained the linear relation  $\log L_{R,39} = (-0.21 \pm 0.08) + (1.08 \pm 0.15) \log L_{X,44}$  for RQQs. In Figure 1, we plot  $L_R$  and  $L_X$  from our 276 samples on log–log coordinates and get a slightly different relation

$$\log L_R = (-9.466 \pm 0.102) + (1.122 \pm 0.002) \log L_X \quad (1)$$

with a correlation coefficient of  $\zeta = 0.980$ ; the  $L_R$  and  $L_X$  are expressed in units of  $\text{erg s}^{-1}$ . For comparison, we have also selected all the 47 GRBs and try to examine the correlation between  $L_R$  and  $L_X$ . The best fitting result is

$$\log L_R = (9.288 \pm 1.339) + (0.695 \pm 0.028) \log L_X \quad (2)$$

with a correlation coefficient of  $\zeta = 0.814$ . We should notice that the range for GRBs is roughly  $10^{40} - 10^{48} \text{erg s}^{-1}$ .

These correlations that are defined by Equations (1) and (2) can be transformed into

$$L_{R,40} \simeq 10.6L_{X,45}^{1.1} \quad \text{and} \quad L_{R,40} \simeq 3.65L_{X,45}^{0.7}. \quad (3)$$

The conventional notation  $Q = Q_k \times 10^k$  is adopted. The correlation defined by Equation (1) is consistent with Laor & Behar (2008) with a slightly different slope. The slope with index 1.1 that includes the GRBs is steeper than the linear correlation. The contribution of the GRBs with slope index  $\sim 0.7$  just extends the whole correlation while maintaining a linear shape. It is interesting to note that the slope of GRBs only is very similar to the slope that corresponds to the X-ray binaries (Gallo et al. 2003).

### 3 CONCLUSIONS AND DISCUSSION

The relation between  $L_R$  and  $L_X$  for GRBs was investigated in this work. We found that the  $L_R - L_X$  correlation that exists for solar flares, cool stars and AGNs can be extended to GRBs. Even

<sup>1</sup> [http://www.swift.ac.uk/xrt\\_products/index.php](http://www.swift.ac.uk/xrt_products/index.php)

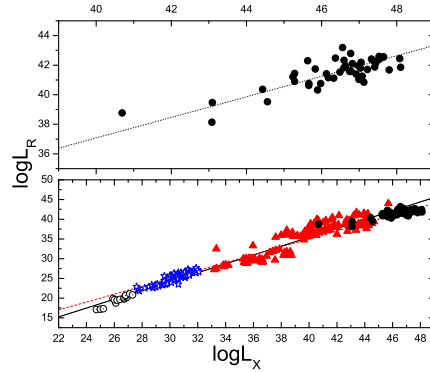


**Fig. 1** The correlation between radio luminosity and X-ray luminosity for a variety of astronomical objects. The upper panel only includes GRBs and their best fitting linear correlation is shown by the black dotted line ( $L_R \simeq 1.94 \times 10^9 L_X^{0.695}$ ), where  $L_R$  and  $L_X$  are in units of  $\text{erg s}^{-1}$ . The lower panel features 15 solar flares (black circles with a dot), 65 cool stars (blue stars), 149 AGNs (red triangles) and 47 GRBs (black solid circles) in the  $L_R - L_X$  plane. The black solid line,  $L_{R,40} \simeq 10.6 L_{X,45}^{1.1}$ , is the best fit. The red dashed line indicates  $L_R = 10^{-5} L_X$ .

though these astrophysical phenomena are divided into different classes, they still have common features as defined by some properties, which implies that they may essentially have some common mechanisms. Franciosini & Chiuderi Drago (1995) presented a model that incorporates a magnetic loop, which only has one free parameter, the thermal plasma density. This approach provides a possible co-spatiality for the two kinds of emissions, radio emission and X-ray emission. On the other hand, the positive correlation between  $L_R$  and  $L_X$  may be more complicated with the detailed underlying nature of this relation still being unclear.

Unlike the other objects, the radio and X-ray data of GRBs were not taken simultaneously. The radio peaks of GRB afterglows are generally observed several days or even months after the burst occurs, but the X-ray data are fixed at 11 hours after the event in the observer's frame. One reason for this is that simultaneous data are very rare. Thanks to the fast response of *Swift* XRT, the X-ray data can be obtained very quickly, but the X-ray emission also decays quickly and fades out in a few days. There is no fast slewing radio telescope that can observe the very early radio emission. Another issue is that the radio emission region is always optically thick in the early stage, and its luminosity is suppressed and is also sensitively related to its size. Therefore, even though the GRB location is occasionally inside the field of view of a radio telescope, it is very hard to detect because of its faint luminosity. Later, after the GRB ejecta has expanded, the radio emission emerges while the X-ray fades away. That means the simultaneous radio and X-ray luminosities may not obey a proportionality relation. From the light curves of GRB X-ray afterglows, the X-ray luminosity at 11 hours generally represents typical X-ray emission. The correlation between the peak radio luminosity and X-ray luminosity at 11 hours may indicate the origin of their energy could be related, rather than arising from microphysical radiation mechanisms. An extension of this behavior to the various objects may also indicate that the radio and X-ray emission could have the same mechanism that radiates in the two different bands.

The fundamental plane between  $L_X$ ,  $L_R$  and  $M_{\text{BH}}$  is even tighter in stellar mass and supermassive black holes (Merloni et al. 2003). Although a GRB is likely to harbor a stellar mass black hole, the fundamental plane does not extend to GRBs.

**Acknowledgements** We thank the referee for careful and enlightening comments and suggestions. This work is supported by the National Natural Science Foundation of China (Grant Nos. U1231101 and 11173011), and the Guangxi Science Foundation (Grant No. 2014GXNSFBA118009).

## References

- Amati, L., Frontera, F., Tavani, M., et al. 2002, *A&A*, 390, 81
- Anderson, G. E., van der Horst, A. J., Staley, T. D., et al. 2014, *MNRAS*, 440, 2059
- Benz, A. O., Gudel, M., & Schmitt, J. H. M. M. 1996, in *Astronomical Society of the Pacific Conference Series*, 93, *Radio Emission from the Stars and the Sun*, eds. A. R. Taylor, & J. M. Paredes, 291
- Benz, A. O., & Guedel, M. 1994, *A&A*, 285, 621
- Chandra, P., & Frail, D. A. 2012, *ApJ*, 746, 156
- Cucchiara, A., Prochaska, J. X., Perley, D., et al. 2013, *ApJ*, 777, 94
- de Ugarte Postigo, A., Xu, D., Malesani, D., et al. 2013, *GRB Coordinates Network*, 15187, 1
- Flores, H., Covino, S., Xu, D., et al. 2013, *GRB Coordinates Network*, 14491, 1
- Fong, W., Berger, E., Metzger, B. D., et al. 2014, *ApJ*, 780, 118
- Franciosini, E., & Chiuderi Drago, F. 1995, *A&A*, 297, 535
- Gallo, E., Fender, R. P., & Pooley, G. G. 2003, *MNRAS*, 344, 60
- Geng, J. J., & Huang, Y. F. 2013, *ApJ*, 764, 75
- Ghirlanda, G., Ghisellini, G., & Lazzati, D. 2004, *ApJ*, 616, 331
- Ghirlanda, G., Nava, L., Ghisellini, G., et al. 2012, *MNRAS*, 420, 483
- Guedel, M. 1996, in *IAU Symposium 176, Stellar Surface Structure*, eds. K. G. Strassmeier, & J. L. Linsky, 485
- Guedel, M., & Benz, A. O. 1993, *ApJ*, 405, L63
- Guedel, M., Schmitt, J. H. M. M., Bookbinder, J. A., & Fleming, T. A. 1993, *ApJ*, 415, 236
- Klebesadel, R. W., Strong, I. B., & Olson, R. A. 1973, *ApJ*, 182, L85
- Kruehler, T., Fynbo, J. P. U., Milvang-Jensen, B., Tanvir, N., & Jakobsson, P. 2012, *GRB Coordinates Network*, 13134, 1
- Kumar, P., & Zhang, B. 2014, arXiv:1410.0679
- Laor, A., & Behar, E. 2008, *MNRAS*, 390, 847
- Lei, W.-H., Zhang, B., & Liang, E.-W. 2013, *ApJ*, 765, 125
- Liang, E.-W., Yi, S.-X., Zhang, J., et al. 2010, *ApJ*, 725, 2209
- Liang, E., & Zhang, B. 2005, *ApJ*, 633, 611
- Linsky, J. L. 1996, in *Astronomical Society of the Pacific Conference Series*, 93, *Radio Emission from the Stars and the Sun*, eds. A. R. Taylor, & J. M. Paredes, 439
- Lü, J., Zou, Y.-C., Lei, W.-H., et al. 2012, *ApJ*, 751, 49
- Merloni, A., Heinz, S., & di Matteo, T. 2003, *MNRAS*, 345, 1057
- Middleton, M. J., Miller-Jones, J. C. A., Markoff, S., et al. 2013, *Nature*, 493, 187
- Piran, T. 2004, *Reviews of Modern Physics*, 76, 1143
- Sanders, D. B., Phinney, E. S., Neugebauer, G., Soifer, B. T., & Matthews, K. 1989, *ApJ*, 347, 29
- Staley, T. D., Titterton, D. J., Fender, R. P., et al. 2013, *MNRAS*, 428, 3114
- van den Oord, G. H. J. 1999, in *Astronomical Society of the Pacific Conference Series*, 158, *Solar and Stellar Activity: Similarities and Differences*, eds. C. J. Butler, & J. G. Doyle, 189
- van der Horst, A. J., Levan, A. J., Pooley, G. G., et al. 2015, *MNRAS*, 446, 4116
- Veres, P., Corsi, A., Frail, D. A., Cenko, S. B., & Perley, D. A. 2014, arXiv:1411.7368
- Wang, F. Y., Yi, S. X., & Dai, Z. G. 2014a, *ApJ*, 786, L8
- Wang, J.-Z., Lei, W.-H., Wang, D.-X., et al. 2014b, *ApJ*, 788, 32
- Wu, Q., Zou, Y.-C., Cao, X., Wang, D.-X., & Chen, L. 2011, *ApJ*, 740, L21
- Xu, D., de Ugarte Postigo, A., Schulze, S., et al. 2013, *GRB Coordinates Network*, 14478, 1
- Xu, M., & Huang, Y. F. 2012, *A&A*, 538, A134
- Yonetoku, D., Murakami, T., Nakamura, T., et al. 2004, *ApJ*, 609, 935
- Zauderer, B. A., Berger, E., Margutti, R., et al. 2013, *ApJ*, 767, 161
- Zhang, B. 2007, *ChJAA (Chin. J. Astron. Astrophys.)*, 7, 1
- Zhang, Z.-B., Kong, S.-W., Huang, Y.-F., Li, D., & Li, L.-B. 2015, *RAA (Research in Astronomy and Astrophysics)*, 15, 237